

# Therapy Related Changes in Osteosarcoma and Ewing Sarcoma of Bone

Hye Sook Min<sup>1</sup>, Hyun Guy Kang<sup>2</sup> and Jae Y. Ro<sup>\*,3</sup>

<sup>1</sup>Department of Pathology and <sup>2</sup>Orthopaedic Surgical Oncology, National Cancer Center, Goyang, Gyeonggido, South Korea; <sup>3</sup>Department of Pathology, Weill Medical College, Cornell University, The Methodist Hospital, Houston, TX 77030, USA

**Abstract:** Histologic evaluation of neoadjuvant chemotherapy effect is a well-established prognostic indicator in osteosarcoma and Ewing sarcoma arising in bone. Although tumor necrosis is a primary histologic response for the treatment, secondary degenerative changes following necrosis are frequently shown in those tumors. We reviewed some cases of Ewing sarcoma and osteosarcoma of bone with variable histologic alterations after chemotherapy. Secondary degenerative changes seemed to be quite diverse; complete coagulative necrosis, fibrosis/hyalinization, vascular enrichment, edematous stroma, variable shapes of bony trabeculae, and cystic/hemorrhagic changes replaced the tumors. Morphologic changes of the primary tumor cells were not prominent. Such recognition of histologic patterns after chemotherapy would be a great help for the evaluation of therapeutic effect.

**Keywords:** Neoadjuvant chemotherapy, histologic response, bone tumors.

## INTRODUCTION

In primary bone tumors including osteosarcoma and Ewing sarcoma, preoperative (neoadjuvant) chemotherapy enables limb-salvage surgery through the reduction of tumor size, and decreases micrometastasis [1-4]. Although magnetic resonance imaging (MRI) and positron emission tomography (PET) sensitively evaluate the chemotherapeutic effect on those bone tumors, histologic evaluation of a post-chemotherapy specimen is generally accepted as the most reliable therapeutic indicator in predicting local recurrence and survival rates. Pathologically more than 90% tumor necrosis is independently associated with a better prognosis in osteosarcoma [3], and also poor chemotherapy-induced necrosis indicated an adverse prognosis in Ewing sarcoma and osteosarcoma [5]. However, chemotherapy induces variable histologic alterations in addition to tumor necrosis. Herein we analyzed histologic response by chemotherapy, in osteosarcomas and Ewing sarcomas arising in the bone.

## MATERIAL AND METHODS

### Case Selection and Pathologic Evaluation

Our study comprises 3 patients of Ewing sarcoma (3 females, aged 5, 20, 29 years, mean age at diagnosis: 18 years) and 5 patients of osteosarcoma (5 females, aged 12-25 years, mean age at diagnosis, 16.4 years). All the patients were initially diagnosed by the incisional biopsy before preoperative chemotherapy, and subsequently underwent chemotherapy and limb-salvage surgery. Neoadjuvant chemotherapy was performed according to the standard protocol. The cycles of VAC/IE (vincristine, actinomycin D,

cyclophosphamide/ifosfamide, etoposide) or VIDE (vincristine, ifosfamide, doxorubicin, etoposide) regimen were used in Ewing sarcoma, and MAP (methotrexate, doxorubicin, cisplatin) regimen was used in osteosarcoma. After surgical resection, all specimens were dissected along the central plane of tumor growth that the greatest extent of tumor could be exposed. Those planes were histologically mapped for the therapeutic evaluation, as in the conventional manner [6]. Microscopically, the percentages of necrosis and other degenerative changes were recorded, and the viable portion was also examined.

## RESULTS

### Ewing Sarcoma (Table 1A)

Tumors were developed from the proximal humerus, rib, and ilium, one each case, encompassing long bone to flat bone. T2-weighted MRI generally showed a mass of mildly to moderately increased signal intensity with irregular enhancement, which accompanied with cortical destruction and soft tissue extension (Fig. 1A, B). The initial needle biopsy of first case demonstrated small round cells with eosinophilic cytoplasm, which were loosely dispersed or vaguely aggregated in small clusters (Fig. 2A). Morphologic, immunohistochemical and fluorescent in situ hybridization (FISH) studies indicated it as Ewing sarcoma (Fig. 2B, C). Although the comparison of pre-chemotherapy and post-chemotherapy radiology only showed a mild reduction of tumor size (Fig. 1), the excised specimen showed grossly visible yellowish necrotic area and pinkish-white solid viable area (Fig. 2D), corresponding to 60% necrosis. Microscopically, a large area of coagulative necrosis with hemosiderin-laden macrophages was observed, and the border between necrosis and viable tissue was sharply delineated (Fig. 2E). The viable tissue contained uniform small round cells with fine chromatin, clear or eosinophilic

\*Address correspondence to this author at the Department of Pathology, Weill Medical College, Cornell University, The Methodist Hospital, 6565 Fannin Street, Houston, TX 77030, USA; Tel: 713-441-2263; Fax: 713-793-1603; E-mail: jaero@tmhs.org

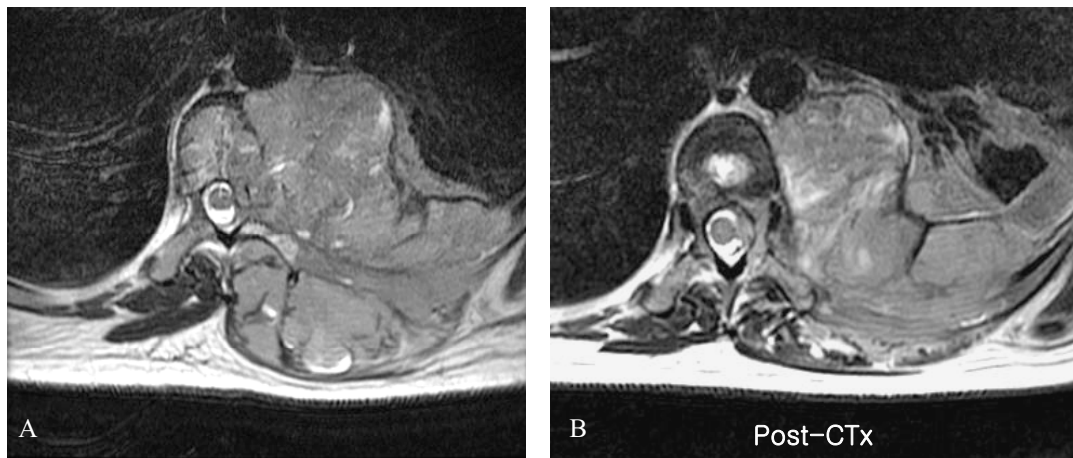


**Fig. (1).** A 29-year-old female's T2-weighted images of spine MRI highlights a huge lobulating mass involving left posterior rib (6th-9th), vertebral column and paravertebral space (A). Through the four-time chemotherapy of \*VAC/IE, the tumor size is mildly reduced (B). \*VAC/IE: vincristine, actinomycin D, cyclophosphamide/ifosfamide, etoposide.

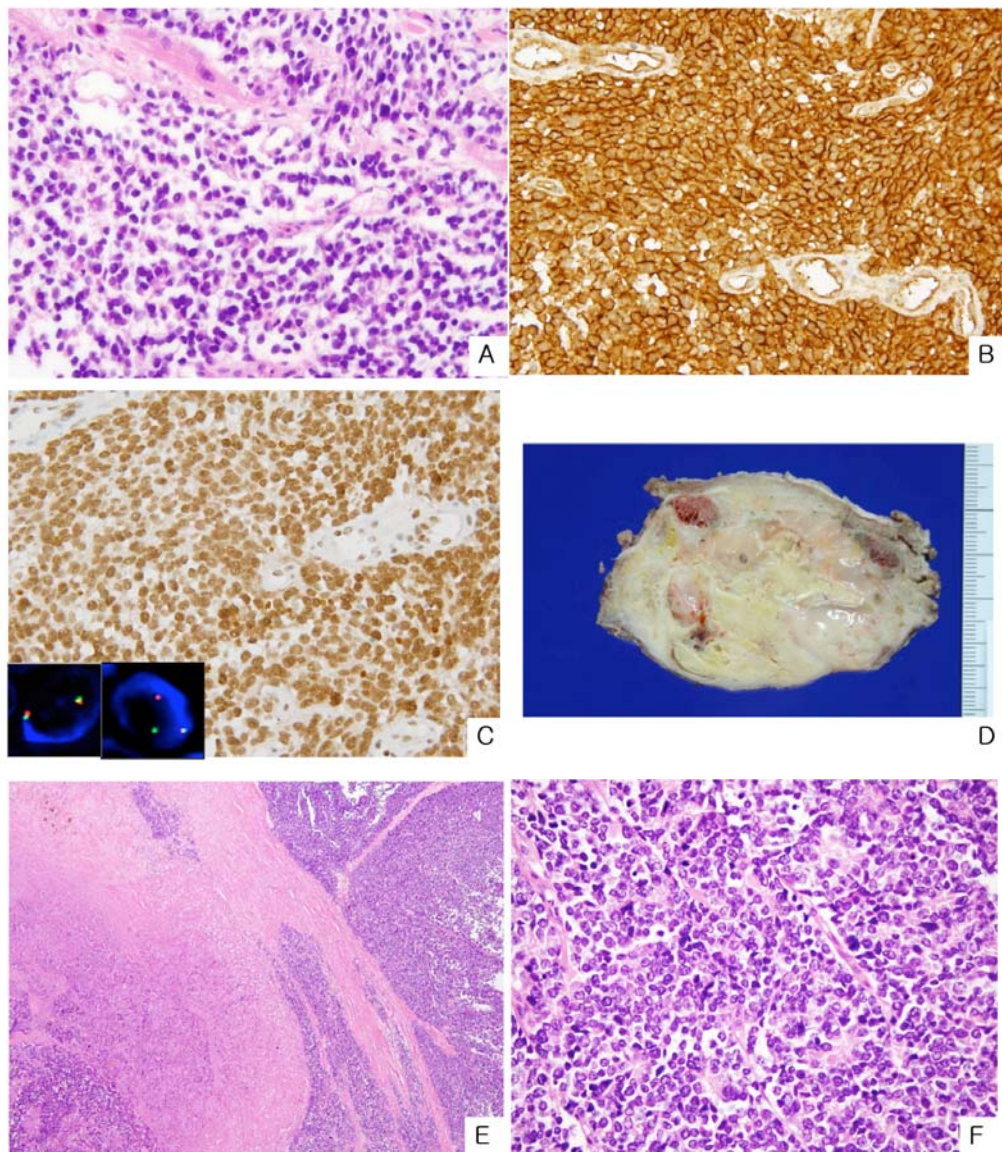


**Fig. (2).** The incisional biopsy contains loosely dispersed small round cells with eosinophilic cytoplasm (A), with strong CD99 (B) and fli-1 (C) positivity and EWS gene rearrangement by fluorescence in situ hybridization (C, inlet). After neoadjuvant chemotherapy, the resected tumor displays large necrotic portion (D) that corresponds to the microscopic finding (E). In a viable portion, the diffuse growth of small round cells with occasional rosette formation are seen (F).

cytoplasm, and rosette formation by fibrillary processes (Fig. 2F). The reparative fibrotic change in chemotherapy-responsive area was visible in the second and the third cases, of which excised specimens displayed gray gelatinous and whitish fibrotic appearances (Fig. 3A, B). The second case contained loose or edematous fibrotic scar tissue replacing the tumor that was heavily endowed with fine and delicate vessels (Fig. 4A). The reactive bone formations of irregular trabeculae were observed actively in the periphery. Only some small irregular-shaped islets of tumor cells were

remained in the corner of fibrosis, infiltrated by some lymphocytes (Fig. 4B). This post-chemotherapy necrotic change extended to 95% of tumor, indicating a good prognostic factor. The richly vascularized necrotic and fibrotic tissue was also seen in the third case that totally replaced the original tumor (responsive area: 100%, Fig. 4C). Some broad bony trabeculae and dilated blood vessels were observed around the fibrosis, and the cortical bone adjacent to the scar tissue was moderately thickened by new bone formation.

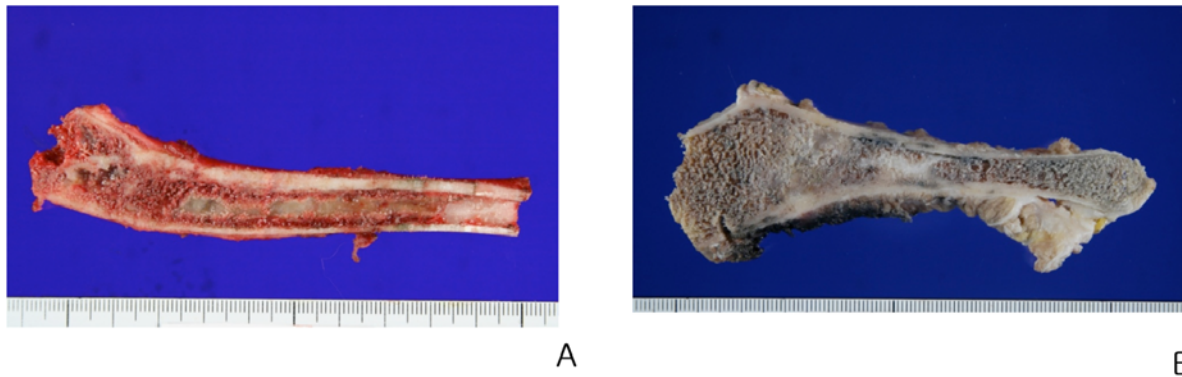


**Fig. (3).** The excised humerus undergone chemotherapy contains a long gelatinous gray area with firm fibrotic portion (A). Another Ewing sarcoma case arising ilium shows irregular whitish lesion with focal cortical thickening after \*VIDE chemotherapy (B). \*VIDE: vincristine, ifosfamide, doxorubicin, etoposide

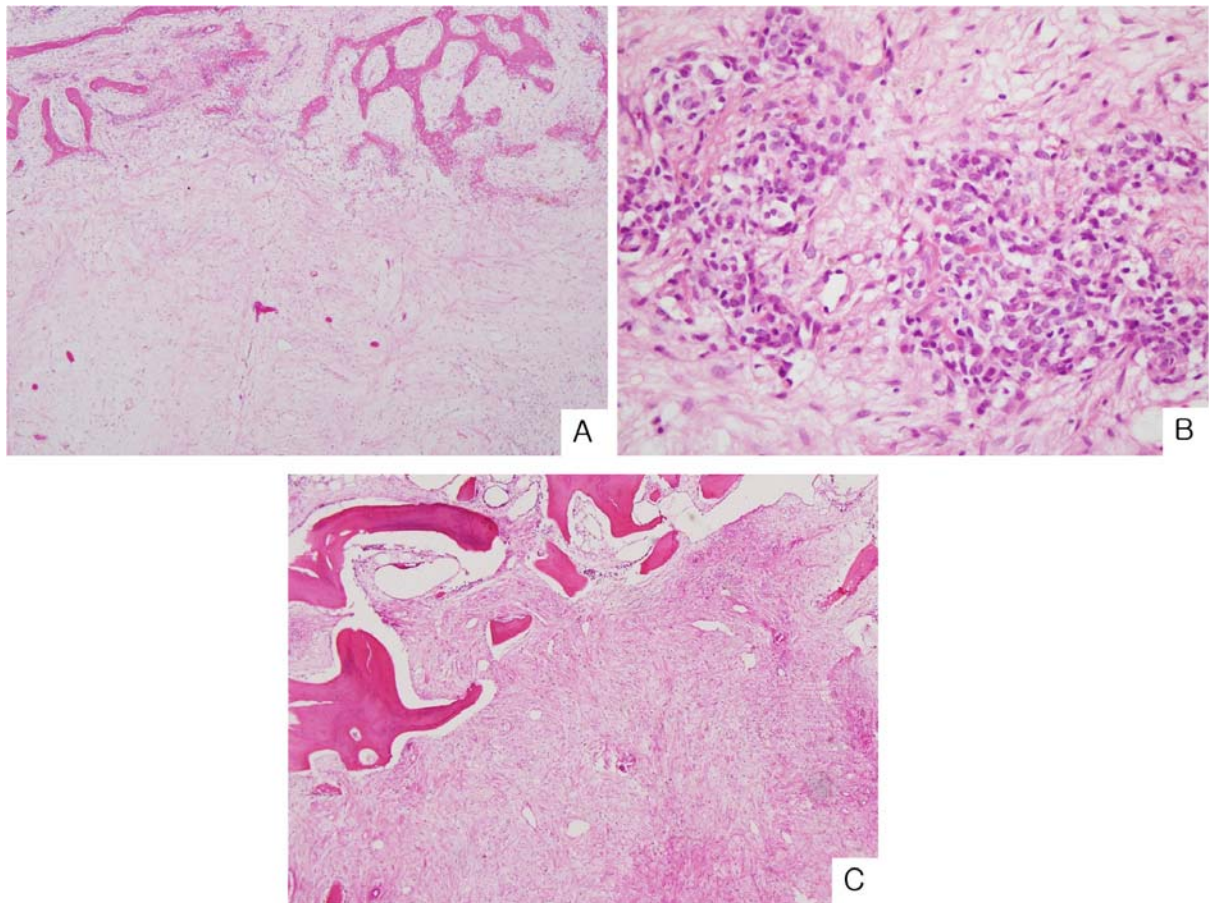


**Fig. (4).** The chemotherapy-responsive area is up to 95% of tumor, of which marrow space is filled with loose fibrotic tissue with reactive bone formation (A). A few remained tumor cell islets are observed in the periphery of fibrosis (B). Another case is totally replaced by fibrotic scar, achieving complete remission (C).

**Table 1A. Cases of Ewing Sarcoma**

Case No.	Age/Sex	Site	Tumor Size	%Necrosis	Metastasis	F/U (Month)
1	29/F	Rib (6 <sup>th</sup> -9 <sup>th</sup> )	8cm	60%	No	DOD* (5 mos)
2	5/F	Proximal humerus	9cm	95%	No	NED <sup>#</sup> (14 mos)
3	20/F	Ilium	4cm	100%	No	NED (30 mos)

DOD\*: Died of disease; NED<sup>#</sup>: No evidence of disease.

**Osteosarcoma (Table 1B)**

Tumors were developed proximal and distal femoral metaphysis and proximal humerus. A plain radiograph of the first case shows a large sclerotic lesion of a 12-year-old female's femoral metaphysis (Fig. 5A), who presented with hip pain for 3 months. The mass showed low signal intensity and the extension to soft tissue in T2-weighted MRI (Fig. 5B). After 3-month chemotherapy, the lesion displayed irregular signal intensity but it seemed to more extend toward diaphysis (Fig. 5C). On gross examination, a huge solid mass was observed showing fish-flesh appearance with multi-lobulating contour (Fig. 5D). Microscopically, the

biopsied tissue before chemotherapy showed conventional osteosarcoma with abundant osteoblastic activity (Fig. 6A). Unfortunately, several times of chemotherapy only induced 10% responsive area in this tumor, which comprised of densely mineralized bony sheets with rich vascular channels (Fig. 6B, C). The majority of tumor cells persisted, and irregularly distributed in the abundant eosinophilic osteoid matrix (Fig. 6D). Another case (Case 5) clearly exhibited similar images and gross findings after chemotherapy (Fig. 7). The distal femoral mass underwent neoadjuvant chemotherapy for 3 months, showing yellowish white firm lesion with irregular border (Fig. 7D). Histologically, loose or edematous hyalinized tissue with only a few benign

**Table 1B. Cases of Osteosarcoma**

Case No.	Age/Sex	Site	Tumor Size	% Necrosis	Metastasis	F/U (Month)
1	12/F	Proximal femur	16 cm	10%	Bone (spine)	AWD* (2 mos)
2	25/F	Distal femur	7 cm	95%	No	NED <sup>#</sup> (5 mos)
3	15/F	Proximal humerus	6 cm	80%	No	NED <sup>#</sup> (10 mos)
4	16/F	Distal femur	8 cm	90%	No	NED <sup>#</sup> (11 mos)
5	14/F	Distal femur	15 cm	40%	Lung	AWD* (20 mos)

AWD\*: alive with disease; NED<sup>#</sup>: No evidence of disease.



**Fig. (5).** A 12-year-old female presented a large sclerotic lesion with irregular periosteal reaction in plain X-ray film, involving the proximal femur (A). T2-weighted MRI delineates the extent of this metaphyseal mass (B) and its more extension toward diaphysis despite 3-month chemotherapy (C). Grossly a 16cm-sized mass filling the medullary cavity shows a white fish-flesh appearance without a visible hemorrhagic or necrotic area. Note that it also extends across the growth plate (D).

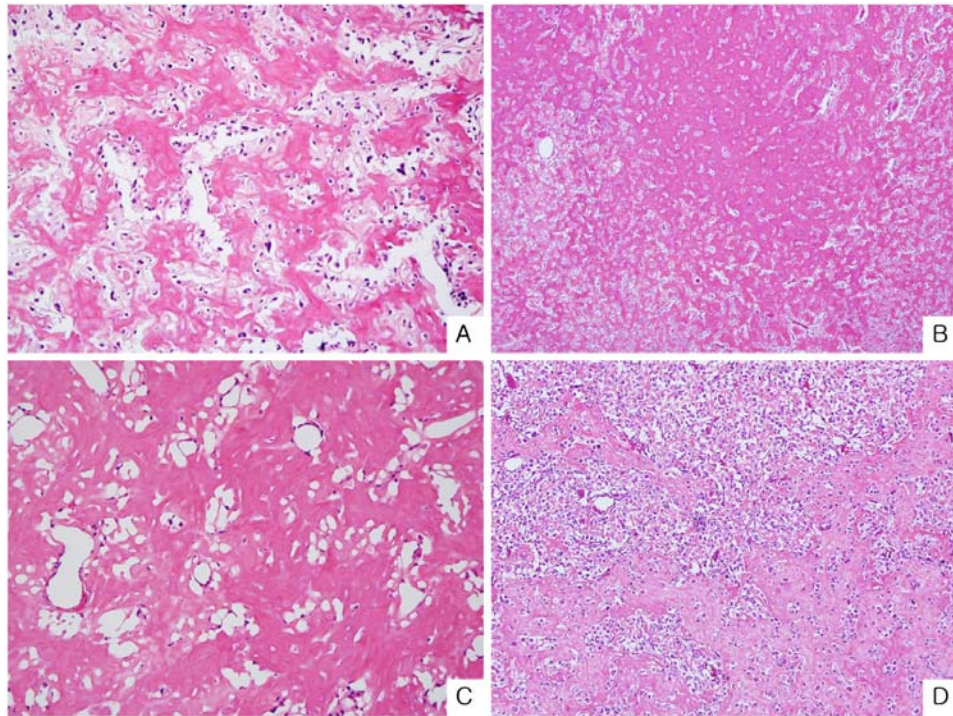


**Fig. (6).** The preoperative biopsy demonstrates osteoblastic osteosarcoma that contains malignant spindle cells with abundant well-formed osteoid matrix (A). The sclerotic sheet-like osteoid matrix with vascular channels is observed after chemotherapy (B, C), and viable tumor cells are remained among abundant eosinophilic matrix (D).

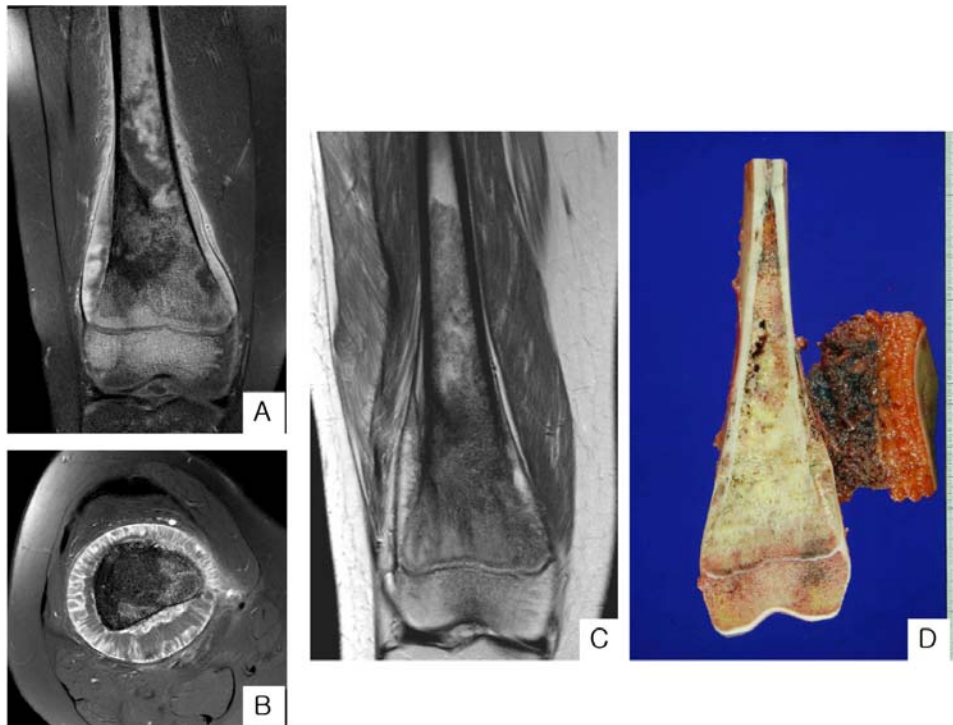


**Fig. (7).** A T2-weighted fat suppressed image of a 14-year-old female showing a bony destructing lesion of mixed signal intensity and sunburst periosteal reaction (A). It totally encircles femoral metaphysis, seen as its axial view (B). The post-chemotherapy image shows mildly reduced periosteal reaction but equivocal tumor size change (C). The excised specimen contains a yellowish white solid lesion with focal hemorrhagic and gelatinous areas (D).

stromal cells or broad sclerotic bony sheets replaced 40% of tumor (Fig. 8A, B). As seen in Fig. (8C-F), variable histological effects by chemotherapy were observed.

**DISCUSSION**

Variable histologic alterations to chemotherapy-responsive tumor have been described only in few articles [1,

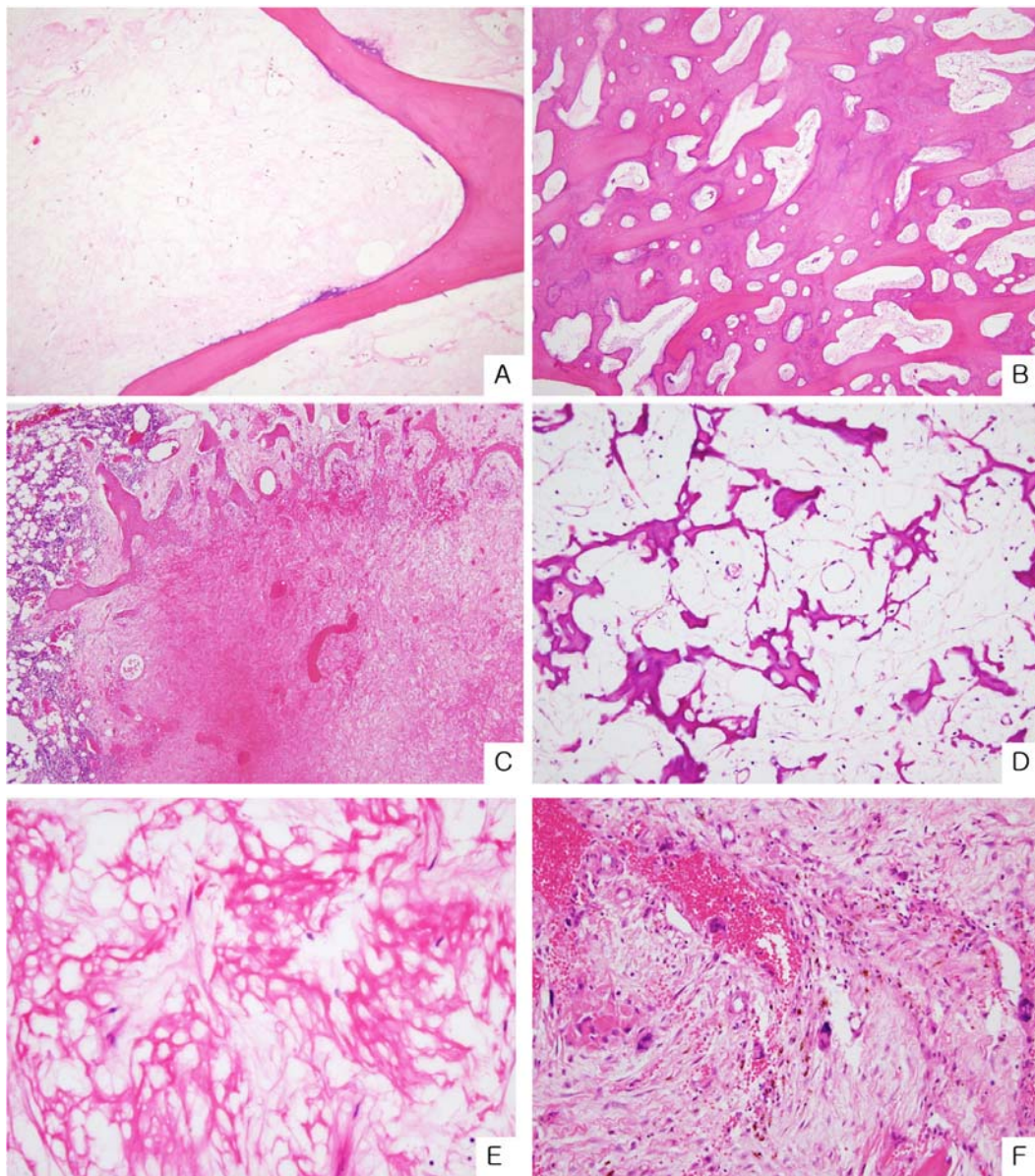


**Fig. (8).** Cases of post-chemotherapy changes. The tumor is replaced by loose fibrotic stroma of scanty cellularity (A) or densely mineralized bony sheets (B). Extensive hemorrhage (C) and some spider-like bony trabeculae in empty-looking stroma are seen (D). In necrotic area, fine ghost-like osteoid matrix is observed with few stromal cells in higher power (E). Sometimes the individual viable tumor cells are found in the chemotherapy-responsive stroma (F).

3, 7, 8]. In the early stage of necrosis, nuclear pyknosis and fragmentation become visible and result in complete elimination of tumor cells, subsequently replaced by a hyalinized vascular stroma. Mucoïd or hemorrhagic cystic change can be acquired [3].

Above cases did not deviate from these descriptions. One Ewing sarcoma case contained complete necrotic area without fibrotic change, indicating relatively acute necrosis before the appearance of reparative process. However, the other two cases displayed copious fibrotic/hyalinized tissue replacing tumor, with reactive bone formation, broad sclerotic bony trabeculae, and cortical thickening. Osteosarcoma cases showed both tumor necrosis and degenerative changes including fibrotic/hyalinized reparative tissue with dense sclerotic osteoid matrix. Pure necrosis and heavy inflammatory cell infiltrations were rarely observed.

These findings have been summarized to three patterns as those of soft tissue sarcoma [7, 8]: the viable tumor, the tumor necrosis and the reparative fibrotic tissue.

In the literature review of osteosarcoma, responsive rates for chemotherapy were significantly different between histologic subtypes, showing a poor histologic response in chondroblastic variant and a good result in telangiectatic type [9, 10]. Pretreated osteosarcomas showed irregularly arranged osteoid matrix, dense or edematous granulation tissue, disorganized fibrotic/collagenous tissue, dystrophic calcification over fibrosis, multicystic change, and hemosiderin deposition [3, 11], most of which were consistent with our findings. Large dilated vessels and marrow infarction were observed in adjacent marrow space [11]. However, the bizarre giant tumor cells with degenerative feature or the activated stromal cells that are

frequently encountered after radiotherapy were not reported. The morphologic feature of both Ewing sarcoma and osteosarcoma tumor cells was not significantly changed after chemotherapy. Although variable histologic alterations by chemotherapy are not expected to influence the prognosis independently [8], the recognition of those histologic patterns should be helpful for the accurate assessment for the remained lesion.

## REFERENCES

- [1] Huvos AG, Rosen G, Marcove RC. Primary osteogenic sarcoma: pathologic aspects in 20 patients after treatment with chemotherapy en bloc resection, and prosthetic bone replacement. *Arch Pathol Lab Med* 1977; 101: 14-8.
- [2] Picci P, Bacci G, Campanacci M, *et al.* Histologic evaluation of necrosis in osteosarcoma induced by chemotherapy. Regional mapping of viable and nonviable tumor. *Cancer* 1985; 56: 1515-21.
- [3] Dorfman H, Czerniak B. *Bone Tumors*. St Louis: Mosby 1998, pp.128-252.
- [4] Bacci G, Picci P, Ferrari S, *et al.* Primary chemotherapy and delayed surgery for nonmetastatic osteosarcoma of the extremities. Results in 164 patients preoperatively treated with high doses of methotrexate followed by cisplatin and doxorubicin. *Cancer* 1993; 72: 3227-38.
- [5] Picci P, Bohling T, Bacci G, *et al.* Chemotherapy-induced tumor necrosis as a prognostic factor in localized Ewing's sarcoma of the extremities. *J Clin Oncol* 1997; 15: 1553-9.
- [6] Raymond AK, Simms W, Ayala AG. Osteosarcoma. Specimen management following primary chemotherapy. *Hematol Oncol Clin North Am* 1995; 9: 841-67.
- [7] MacVicar AD, Olliff JF, Pringle J, *et al.* Ewing sarcoma: MR imaging of chemotherapy-induced changes with histologic correlation. *Radiology* 1992; 184: 859-64.
- [8] Lucas DR, Kshirsagar MP, Biermann JS, *et al.* Histologic alterations from neoadjuvant chemotherapy in high-grade extremity soft tissue sarcoma: clinicopathological correlation. *Oncologist* 2008; 13: 451-8.
- [9] Bacci G, Balladelli A, Palmerini E, *et al.* Neoadjuvant chemotherapy for osteosarcoma of the extremities in preadolescent patients: The Rizzoli Institute experience. *J Pediatr Hematol Oncol* 2008; 30: 908-12.
- [10] Bacci G, Mercuri M, Longhi A, *et al.* Grade of chemotherapy-induced necrosis as a predictor of local and systemic control in 881 patients with non-metastatic osteosarcoma of the extremities treated with neoadjuvant chemotherapy in a single institution. *Eur J Cancer* 2005; 41: 2079-85.
- [11] Pan G, Raymond AK, Carrasco CH, *et al.* Osteosarcoma: MR imaging after preoperative chemotherapy. *Radiology* 1990; 174: 517-26.

Received: June 15, 2009

Revised: June 25, 2009

Accepted: July 5, 2009

© Min *et al.*; Licensee Bentham Open.

This is an open access article licensed under the terms of the Creative Commons Attribution Non-Commercial License (<http://creativecommons.org/licenses/by-nc/3.0/>) which permits unrestricted, non-commercial use, distribution and reproduction in any medium, provided the work is properly cited.